

# Analysis of Phosphorylated Sphingolipid Long-Chain Bases Reveals Potential Roles in Heat Stress and Growth Control in *Saccharomyces*

MAREK S. SKRZYPEK, M. MAREK NAGIEC, ROBERT L. LESTER, AND ROBERT C. DICKSON\*

*Department of Biochemistry and Lucille P. Markey Cancer Center, University of Kentucky Medical Center, Lexington, Kentucky 40536-0298*

Received 18 May 1998/Accepted 30 November 1998

**Sphingolipid long-chain bases and their phosphorylated derivatives, for example, sphingosine-1-phosphate in mammals, have been implicated as signaling molecules. The possibility that *Saccharomyces cerevisiae* cells also use long-chain-base phosphates to regulate cellular processes has only recently begun to be examined. Here we present a simple and sensitive procedure for analyzing and quantifying long-chain-base phosphates in *S. cerevisiae* cells. Our data show for the first time that phytosphingosine-1-phosphate (PHS-1-P) is present at a low but detectable level in cells grown on a fermentable carbon source at 25°C, while dihydro sphingosine-1-phosphate (DHS-1-P) is only barely detectable. Shifting cells to 37°C causes transient eight- and fivefold increases in levels of PHS-1-P and DHS-1-P, respectively, which peak after about 10 min. The amounts of both compounds return to the unstressed levels by 20 min after the temperature shift. These data are consistent with PHS-1-P and DHS-1-P being signaling molecules. Cells unable to break down long-chain-base phosphates, due to deletion of *DPL1* and *LCB3*, show a 500-fold increase in PHS-1-P and DHS-1-P levels, grow slowly, and survive a 44°C heat stress 10-fold better than parental cells. These and other data for *dpl1* or *lcb3* single-mutant strains suggest that DHS-1-P and/or PHS-1-P act as signals for resistance to heat stress. Our procedure should expedite experiments to determine how the synthesis and breakdown of these compounds is regulated and how the compounds mediate resistance to elevated temperature.**

Sphingoid long-chain bases are gaining appreciation for their role in cellular signaling processes. Sphingosine, the primary long-chain base found in mammalian sphingolipids, was first noted for its mitogenic activity (reviewed in references 26 and 27), at least some of which is mediated by sphingosine-1-phosphate (SPP) (31), a phosphorylated derivative of sphingosine. SPP has been shown also to inhibit cell motility and invasiveness of tumor cells (1, 25, 28, 30). Recently SPP and sphingosylphosphorylcholine have been found to bind G-protein-coupled receptors that may play roles in regulating heart rate, the oxidative burst, neurite retraction, and platelet activation (reviewed in reference 32). Most of these observations have been made for cultured cells, and it remains to be determined how physiologically important SPP and related molecules are in whole animals. To begin to assess the physiological role of long-chain-base phosphates in regulating cellular processes, we have determined which compounds are present before and during a heat shock in wild-type *Saccharomyces cerevisiae* cells and in mutant cells defective in breakdown of these compounds.

Studies of mutant *S. cerevisiae* strains lacking sphingolipids indicated an essential role for these lipids in resisting heat, osmotic, and low-pH stresses (22). Further analysis during heat stress indicated that sphingolipids were not necessary for induction of the major heat shock proteins but were necessary for accumulation of trehalose (6), a disaccharide known to be induced by heat stress and to be necessary for full thermoprotection of log-phase (5) and stationary-phase (8) cells. In addition, heat shock induced a 2- to 3-fold transient increase in

the concentration of C<sub>18</sub>-dihydro sphingosine (DHS) and C<sub>18</sub>-phytosphingosine (PHS), more than a 100-fold transient increase in C<sub>20</sub>-DHS and C<sub>20</sub>-PHS, and a stable 2-fold increase in ceramide containing C<sub>18</sub>-PHS and a 5-fold increase in ceramide containing C<sub>20</sub>-PHS (6, 12, 29). Finally, it was shown that treatment of cells with DHS or PHS induced transcription of a reporter gene containing either the *TPS2* promoter or seven copies of the global response element, *STRE*. Transcription of *TPS2*, encoding a subunit of trehalose synthase, has been shown to be induced by several stresses including heat, and the promoter element responsible for these responses has been shown to be *STRE* (9, 13, 18). These results suggest that DHS, PHS, or a derivative thereof can act as a signal to induce transcription.

To further characterize the function of long-chain-base phosphates, we have developed, as described in this report, a quantitative method for their analysis in *S. cerevisiae* cells. Using this method, we show for the first time that *S. cerevisiae* cells have a low basal level of PHS-1-P and a barely detectable level of DHS-1-P. Heat shock induces a rapid but transient increase in the concentration of both compounds, suggesting that they have the potential to be signaling molecules. Analysis of mutant cells unable to breakdown long-chain-base phosphates reveals a large accumulation of both DHS-1-P and PHS-1-P in log-phase cells. This accumulation of long-chain-base phosphates correlates with increased survival at an elevated temperature, suggesting that long-chain-base phosphates may normally play a role in heat stress resistance. Alternative explanations of our data are discussed.

## MATERIALS AND METHODS

**Strains and media.** Strains used in this work are described in Table 1. Strain MSS201 is a Leu<sup>+</sup> derivative of MSS200 made by transformation with the *LEU2* allele and selection for Leu<sup>+</sup> cells. Strain MSS207 is a derivative of MSS200 made by deleting *DPL1* with the  $\Delta 1$  allele (*LEU2* replaces the region between

\* Corresponding author. Mailing address: Department of Biochemistry, University of Kentucky Medical Center, Lexington, KY 40536-0298. Phone: (606) 323-6052. Fax: (606) 257-8940. E-mail: bobd@pop.uky.edu.

TABLE 1. Genotypes of strains used in this work

Strain	Genotype	Description	Reference
Jk9-3da	<i>MATa leu2-3,112 ura3-52 rme1 trp1 his4</i>	Parental strain	11
MSS200	<i>MATa leu2-3,112 ura3-52 rme1 trp1 his4</i> <i>TPS2-lacZ::URA3</i>	Derived from Jk9-3da by integration of <i>TPS2::lacZ</i>	6
MSS201	<i>MATa ura3-52 rme1 trp1 his4</i> <i>TPS2-lacZ::URA3</i>	Derived from MSS200, <i>leu2-3, 112</i> allele repaired with <i>LEU2</i>	This work
MSS204	<i>MATa leu2-3,112 ura3-52 rme1 trp1 his4</i> <i>TPS2-lacZ::URA3 dpl1-Δ1::LEU2</i>	Derived from MSS200, <i>DPL1</i> replaced with <i>LEU2</i>	This work
MSS205	<i>MATa leu2-3,112 ura3-52 rme1 trp1 his4</i> <i>TPS2-lacZ::URA3 lcb3-Δ1::LEU2</i>	Derived from MSS200, <i>LCB3</i> replaced with <i>LEU2</i>	This work
MSS207	<i>MATa leu2-3,112 ura3-52 rme1 trp1 his4</i> <i>TPS2-lacZ::URA3 dpl1-Δ1::leu2::TRP1</i> <i>lcb3-Δ1::LEU2</i>	Derived from MSS204, <i>dpl1-Δ1::LEU2</i> disrupted with <i>TRP1</i> and <i>LCB3</i> replaced with <i>LEU2</i>	This work

the *NheI* and *BglII* restriction sites [codons -10 to 536]), inserting *TRP1* into *LEU2* by a swapping technique (3), and then deleting *LCB3* with the  $\Delta 1$  allele (*LEU2* replaces 522 bp between the *BamHI* and *NsiI* sites) (23). The composition of PYED medium has been described elsewhere (20).

**Analysis of long-chain-base phosphates.** Lipids were uniformly labeled with  $^{32}\text{P}_i$  by growing yeast cells from 0.003 to 0.3  $A_{600}$  units in PYED medium from which the phosphate had been omitted. The medium was supplemented with [ $^{32}\text{P}$ ]H<sub>3</sub>PO<sub>4</sub> (0.1 mCi/ml; ICN, Costa Mesa, Calif.). Prior to lipid extraction, 5 ml of radiolabeled cells was mixed with 50  $A_{600}$  units (4.5 ml) of nonradioactive carrier cells and treated with 5% trichloroacetic acid (0.5 ml of 100%) on ice for 30 min. The sample was centrifuged at 5,000  $\times$  g; the pellet was washed three times with 10 ml of ice-cold 5% trichloroacetic acid and then once with cold water. Residual liquid was carefully removed before extraction of total lipids by a 30-min incubation at 60°C with 0.5 ml of solvent A (95% ethanol, water, diethyl ether, pyridine, concentrated ammonium hydroxide [15:15:5:1:0.018, vol/vol] (10)). The sample was centrifuged in a microcentrifuge at 13,000  $\times$  g before cooling. The supernatant fluid was dried under a stream of nitrogen.

Glycerophospholipids were deacylated by treatment of the sample with 0.5 ml of the monomethylamine reagent for 1 h at 50°C (2). The sample was dried under a stream of nitrogen. The remaining lipids were dissolved in 0.5 ml of solvent A lacking ammonia.

To separate most sphingolipids and other unknown radiolabeled compounds from the long-chain-base phosphates, the lipid extract was applied to a 1-ml AG4-X4 (200/400 mesh; Bio-Rad, Hercules, Calif.) ion-exchange column which had been washed with 1 ml of water and 1 ml of methanol before equilibration with 3 ml of solvent A lacking ammonia. After loading the sample, the column was washed five times with 0.5 ml of solvent A lacking ammonia, followed by elution with 0.5-ml volumes of solvent A lacking ammonium hydroxide but acidified with glacial acetic acid (4  $\mu\text{l}/\text{ml}$ ). The 10 fractions were monitored, and those containing the small radioactive peak, usually fractions 6 and 7, were combined. This elution schedule was derived from pilot experiments in which [ $^3\text{H}$ ]DHS-1-P, mixed with a nonradioactive lipid extract and deacylated, was eluted with lipid extraction solvent containing increasing amounts of acid. Under the conditions described, more than 99% of the [ $^3\text{H}$ ]DHS-1-P eluted from the column.

The combined fractions were dried under a stream of nitrogen, resuspended in 0.5 ml of solvent A, and chromatographed on thin-layer chromatography (TLC) plates (K5 Silica Gel 100A; Whatman, Clifton, N.J.) in solvent B (chloroform, methanol, water [60:35:8]) or solvent C (chloroform, methanol, 4.2 N ammonium hydroxide [9:7:2]) as indicated. Radioactivity was localized and quantified by using a PhosphorImager (Molecular Dynamics, Sunnyvale, Calif.).

**Synthesis of  $^{32}\text{P}$ -labeled long-chain-base phosphates.** Soluble yeast proteins were prepared by vortexing (6 30-s bursts in a 15-ml Corex tube) 50  $A_{600}$  units of yeast cells in 1 ml of the extraction buffer (50 mM HEPES [pH 7.5], 5 mM dithiothreitol, 1 mM phenylmethylsulfonyl fluoride, and 1 mg each of leupeptin, pepstatin, and aprotinin per ml) with 0.5 ml of 0.5-mm-diameter acid-washed glass beads. This and all other steps were done at 4°C. The lysate was centrifuged for 5 min at 1,000  $\times$  g, and the resulting supernatant fluid was centrifuged at 100,000  $\times$  g for 15 min in a TLA 100.3 rotor (Beckman). The final supernatant fluid, containing soluble yeast proteins, was frozen and stored at -20°C and then thawed at 4°C for use in long-chain-base kinase assays.

The long-chain-base kinase assay was based on the method of Crowther and Lynch (4). Reaction mixtures contained 12  $\mu\text{M}$  DL-erythro [4,5- $^3\text{H}$ ]DHS (35,000 cpm), 0.5 mM Triton X-100, 1 mM MgCl<sub>2</sub>, 1 mM ATP, 100 mM Tricine (pH 8.1), and 2 to 50  $\mu\text{g}$  of soluble yeast proteins in a total volume of 100  $\mu\text{l}$ . After incubation at 30°C for 30 min, the product was separated from the substrate by differential solvent extraction exactly as described previously (4). The amount of product formed was determined by liquid scintillation counting in Ultima Gold LSC-cocktail (Packard). The Bradford reagent (Bio-Rad Laboratories) was used to measure protein concentrations, with bovine serum albumin as a standard.

Synthesis of  $^{32}\text{P}$ -labeled long-chain-base phosphates was done by using the

same reaction conditions as described above except that nonradioactive long-chain base was used and the reaction mixture contained 10  $\mu\text{Ci}$  of [ $\gamma$ - $^{32}\text{P}$ ]ATP (4,500 Ci/mmol; ICN). The reaction was stopped by addition of 1.28 ml of chloroform-methanol (1:1), and the mixture was used directly for TLC or the long-chain-base phosphate was purified by using an AG4 column as described above.

**Heat stress.** Cells were grown overnight at 25°C in PYED medium to an  $A_{600}$  of 0.3 and then transferred to a 44°C water bath shaker. Viability was determined by diluting samples in distilled water and plating on PYED plates. Colonies were counted after 2 to 6 days incubation at 30°C.

## RESULTS

**Synthesis of long-chain-base phosphates.** Both DHS and PHS are intermediates in yeast sphingolipid biosynthesis, and it is possible that both can be phosphorylated in *S. cerevisiae*. Since radioactive standards for these long-chain-base phosphates are not commercially available, we prepared them by incubating soluble yeast proteins, a robust source of long-chain-base kinase activity, with a nonradioactive long-chain base and [ $\gamma$ - $^{32}\text{P}$ ]ATP. The radioactive products were partially purified on an AG4 column and analyzed by TLC. DL-erythro-DHS and D-erythro-sphingosine gave rise to a radioactive product that chromatographed like the authentic phosphorylated nonradioactive standards (Fig. 1). Substituting PHS for DHS in the reaction produced radioactive PHS-1-P (Fig. 1). The

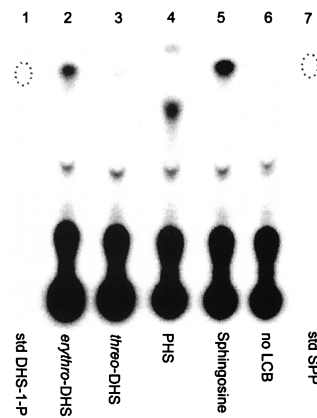


FIG. 1. Synthesis of radioactive long-chain-base phosphates by soluble yeast proteins. Long-chain bases (12  $\mu\text{M}$ ) including DL-erythro-DHS (lane 2), L-threo-DHS (lane 3), PHS (lane 4), and D-erythro-sphingosine (lane 5) were incubated separately with [ $\gamma$ - $^{32}\text{P}$ ]ATP, and soluble proteins were derived from strain MSS200 as described in Materials and Methods. The reaction mixtures were analyzed directly by TLC using solvent C. The locations of nonradioactive standards (std) for DHS-1-P (lane 1) and SPP (lane 7), identified by charring the plate, are indicated by dotted ovals.

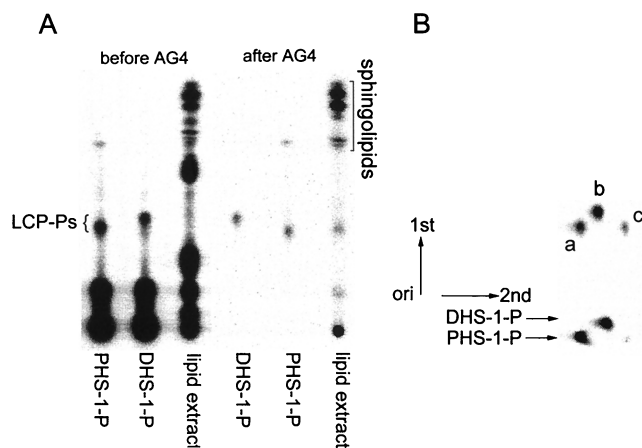


FIG. 2. Chromatographic analysis of long-chain-base phosphates (LCP-Ps). (A) DHS-1-P and PHS-1-P standards, made as described for Fig. 1, and a lipid extract from MSS200 cells were analyzed by TLC using solvent B before or after chromatography on an AG4 column. All samples were radiolabeled with  $^{32}\text{P}$ . (B) DHS-1-P and PHS-1-P standards, purified by chromatography on an AG4 column, were combined and separated by two-dimensional TLC using solvent B in the first dimension and solvent C in the second. Purified DHS-1-P and PHS-1-P standards were also run in the second dimension, as indicated at the bottom. Spots: a and c, PHS-1-P; b, DHS-1-P.

reaction is stereospecific because *L-threo*-DHS was poorly phosphorylated (Fig. 1, lane 3). The minor, rapidly moving product at the top of lane 4 is an uncharacterized derivative produced from PHS during processing (see below).

Treatment of phosphorylated long-chain bases with bacterial alkaline phosphatase released  $^{32}\text{P}_i$  with a concomitant disappearance of the starting compound (data not shown), indicating that the phosphate was present in a phosphomonoester linkage, as expected for a long-chain-base phosphate. We conclude from these results that radioactive long-chain-base phosphates can be made with the reaction conditions described above.

**Method for measurement of long-chain-base phosphates.** Currently there is no simple and quantitative procedure for measuring long-chain-base phosphates in *S. cerevisiae* cells. Therefore, we sought to develop a simple procedure that used an inexpensive radiolabel to quantify and characterize all long-chain-base phosphates present in *S. cerevisiae* cells.

Cells were grown several generations in the presence of  $^{32}\text{P}_i$  to radiolabel all phosphorylated compounds to equilibrium. Lipids were extracted as described in Materials and Methods. Analysis of the deacylated lipid fraction by TLC did not clearly indicate the presence of long-chain-base phosphates because of a smear of radioactivity migrating where PHS-1-P and DHS-1-P were expected to migrate (Fig. 2A, before AG4).

To enrich for long-chain-base phosphates, we developed a procedure using anion-exchange chromatography on AG4 resin, with the loading solvent having a slightly alkaline pH and the eluting solvent having an acid pH. The rationale for this approach is that the long-chain-base phosphates should be slightly negatively charged at alkaline pH whereas at a lower pH they become zwitterionic with no net charge. Thus, they should elute from the column while most of the acidic phospholipids should not. Neutral lipids and lipid derivatives containing phosphocholine and phosphoethanolamine should not bind to the resin and should not interfere with subsequent analysis by TLC. This rationale was verified experimentally. When a radiolabeled lipid extract was chromatographed on the AG4 column and the fractions containing long-

chain-base phosphates were analyzed by TLC, there was nearly a 100-fold enrichment for long-chain-base phosphates, and they were well separated from the small amount of sphingolipids and other unidentified compounds that eluted from the column (Fig. 2A, after AG4). We also measured the percentage of DHS-1-P and PHS-1-P recovered during these enrichment steps. A known number of counts per minute of each pure  $^{32}\text{P}$ -labeled compound was added to the crude lipid extract prepared from wild-type cells. The samples were processed, chromatographed on an AG4 column, and analyzed by one-dimensional TLC. More than 99% of each lipid was recovered (data not shown).

Since the radiolabeled DHS-1-P and PHS-1-P standards were not well separated by the one-dimensional TLC procedure (Fig. 2A), it would be impossible to determine which species were present in cells. Separation of DHS-1-P (Fig. 2B, spot b) and PHS-1-P (Fig. 2B, spot a) was achieved by developing the TLC in a second dimension, using an alkaline solvent. However, there was a second radioactive spot (Fig. 2B, spot c; see also the PHS-1-P standard at the bottom of Fig. 3A and B) created in the PHS-1-P standard that migrates faster than PHS-1-P.

We examined the origin of spot c in more detail to verify that it arose from PHS-1-P. PHS-1-P was chromatographed in the first dimension, eluted, and analyzed by two-dimensional TLC. Two radioactive species, corresponding to spots a and c, were observed (data not shown). The species corresponding to PHS-1-P (spot a) was eluted and again analyzed by two-dimensional TLC. This time there were three radioactive species (data not shown) corresponding to spots a, c, and d, as indicated in Fig. 3B. We conclude from this experiment and those shown in Fig. 2 that a small amount of PHS-1-P is sometimes converted to a faster-migrating species during the first dimension of the TLC analysis and, following chromatography in the second dimension, gives rise to species d (Fig. 3B). A larger amount of the unknown is formed from PHS-1-P during the second dimension of the TLC procedure, and it gives rise to species c. Thus, the concentration of PHS-1-P is the sum of the radioactive species labeled a, c, and d. We do not know the exact identity of compounds c and d, but they could be a cyclic phosphate derivative of PHS-1-P.

**Types of long-chain-base phosphates present in *S. cerevisiae* cells.** To determine the types of long-chain-base phosphates present in wild-type *S. cerevisiae* cells, we grew cells in the presence of  $^{32}\text{P}$  and extracted and processed the lipids as described in Materials and Methods. The two-dimensional TLC separation procedure revealed the presence of PHS-1-P (Fig. 3A, spots a and c) and almost no DHS-1-P (Fig. 3A, spot b) in log-phase cells grown at 25°C on complex medium having glucose as the carbon source.

**Long-chain-base phosphates transiently increase during heat stress.** If long-chain-base phosphates play a role in signal transduction during heat stress, their concentration should change after cells are shifted from a nonstressful to a stressful temperature. To determine if this was the case, we measured the quantity and type of long-chain-base phosphates in cells grown at 25°C and after a shift to 37°C.

At the earliest time point analyzed after the temperature shift, 5 min, we observed increases in PHS-1-P (Fig. 3B, spots a, c, and d) and DHS-1-P (Fig. 3B, spot b). Samples taken at all time points in this experiment were analyzed by two-dimensional TLC, and radioactivity was quantified by PhosphorImager analysis. At their peaks, which occurred around 10 min after the temperature shift, the concentrations of PHS-1-P and DHS-1-P were eight- and fivefold, respectively, above the baseline levels (Fig. 3C). The levels of both long-chain-base phosphates



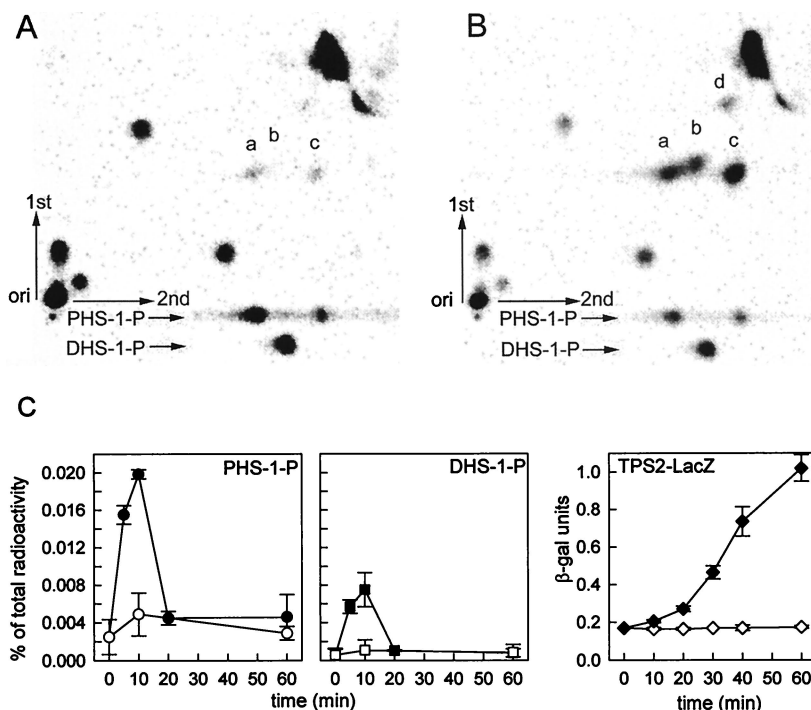


FIG. 3. PHS-1-P and DHS-1-P transiently increase during heat stress, as determined by analysis of  $^{32}\text{P}$ -labeled long-chain-base phosphates present in MSS200 cells grown in PYED medium at 25°C (A) or following a shift to 37°C (B). Cells were radiolabeled, and lipids were extracted and processed as described in Materials and Methods. Lipids were separated by two-dimensional TLC with solvent B used first and solvent C used second. Purified DHS-1-P and PHS-1-P standards were also run in the second dimension as indicated at the bottom. Spots: a, c, and d, PHS-1-P; b, DHS-1-P. (C) Lipid extracts were prepared at various times from cells grown at 25°C (open symbols) or following transfer to 37°C at time zero (filled symbols). The amount of radioactivity in DHS-1-P (spot a) and PHS-1-P (sum of spots b, c, and d) was quantified in each sample by using a PhosphorImager and expressed as a percentage of the counts present in the total lipid extract. The rightmost panel shows the amount of  $\beta$ -galactosidase activity in the cells grown at 25°C (open diamonds) or 37°C (filled diamonds). Data are the means  $\pm$  standard deviations for two experiments.

phates returned to the uninduced levels by about 20 min even though the cells were still growing at 37°C.

We previously suggested that one process regulated by DHS, PHS, ceramide, or derivatives of them is transcriptional activation of the *TPS2* gene (6). To determine if long-chain-base phosphates are components of a signaling pathway leading to induction of *TPS2* transcription, we measured the kinetics of *TPS2* transcription activation following a shift of cells from 25 to 37°C. Induction of *TPS2* transcription was monitored by using a *TPS2-lacZ* reporter gene and measuring  $\beta$ -galactosidase activity.  $\beta$ -Galactosidase activity began to increase at about 10 min after the temperature shift (Fig. 3C). These kinetics are consistent with one or more long-chain-base phosphate acting as a signal to activate transcription of *TPS2*.

#### Long-chain-base phosphates accumulate in mutant strains.

To further understand the function of long-chain-base phosphates in *S. cerevisiae*, we deleted genes necessary for their catabolism. We anticipated that if there is a flux through long-chain-base phosphates, then deletions might disrupt the flux and cause accumulation of either or both intermediates. Analysis of phenotypes might suggest functions for long-chain-base phosphates. The genes deleted were *DPL1* (see Fig. 6), necessary for long-chain-base phosphate lyase activity (24), and *LCB3*, necessary for the majority of phosphatase activity that dephosphorylates long-chain-base phosphates in yeast cells (16, 17).

The *dpl1* deletion mutant (strain MSS204) had a 24-fold increase in the basal level of PHS-1-P but no increase in DHS-1-P; there was no detectable DHS-1-P (Fig. 4, time zero). The *lcb3* deletion mutant (strain MSS205) had a 28-fold increase in the basal level of PHS-1-P and a 43-increase in the basal level

of DHS-1-P (Fig. 4, time zero). The *dpl1 lcb3* double mutant (strain MSS207) had more than a 500-fold increase in total long-chain-base phosphates, there being slightly more DHS-1-P than PHS-1-P (Fig. 4, time zero). These data suggest that there is a flux through DHS-1-P and PHS-1-P and that the *Dpl1* lyase and *Lcb3* phosphatase activities play roles in maintaining the basal rate of flux.

Because of nonradioactive phosphate in the culture medium, it is not possible to determine the specific activity of the  $^{32}\text{P}_i$  radiolabel, which prevents us from determining the concentration of PHS-1-P and DHS-1-P. What can be measured are their concentrations relative to other radiolabeled lipids. Together, DHS-1-P and PHS-1-P account for only 0.0046% of the  $^{32}\text{P}$  in the total lipid extract, showing that they are present at a very low level in log-phase cells grown at 25°C in PYED medium.

Since a shift of wild-type cells from 25 to 37°C causes a transient increase in both DHS-1-P and PHS-1-P (Fig. 3), we examined the mutant strains for a similar behavior. A 10-min heat treatment produced an increase in PHS-1-P over the basal level in the *dpl1* mutant (Fig. 4, strain MSS204), with the level decreasing after 40 min. Heat treatment did not induce DHS-1-P accumulation in this strain. Heat treatment produced only a very small increase in PHS-1-P in the *lcb3* mutant, but DHS-1-P was transiently increased two- to threefold (Fig. 4). Heat treatment produced no measurable change in the level of either DHS-1-P or PHS-1-P in the *dpl1 lcb3* double mutant (Fig. 4). These data demonstrate that there is a complex set of heat-induced changes in long-chain-base phosphates that is unique to each mutant strain and to wild-type cells.

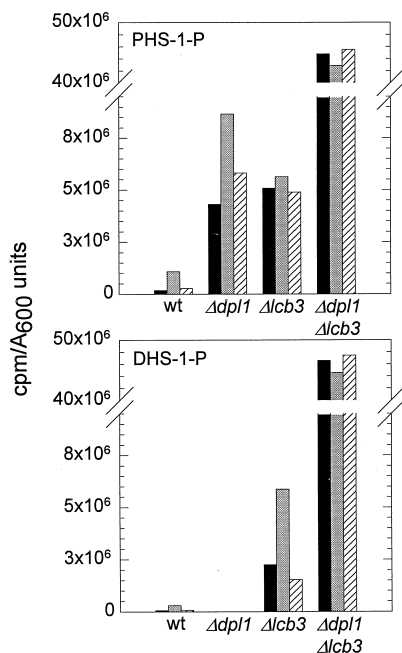


FIG. 4. Analysis of long-chain-base phosphates in wild-type (wt) strain MSS201 and mutant strains MSS204 ( $\Delta dpl1$ ), MSS205 ( $\Delta lcb3$ ), and MSS207 ( $\Delta dpl1 \Delta lcb3$ ). The types and amounts of  $^{32}\text{P}$ -labeled long-chain-base phosphates present in log-phase cells grown at 25°C (time zero; black bars) and after 10 min (gray bars) and 40 min (cross-hatched bars) of incubation at 37°C were analyzed by two-dimensional TLC using solvent B in the first dimension and solvent C in the second dimension. Spots corresponding to PHS-1-P (top) and DHS-1-P (bottom) were quantified by PhosphorImager analysis of the TLC plate and are represented on the y axis. Purified PHS-1-P and DHS-1-P standards were run for comparison.

**Mutant strains are more heat resistant.** The *dpl1* (strain MSS204) and *lcb3* (strain MSS205) single-deletion mutants grew normally in rich or synthetic medium at 25, 30, and 37°C. In contrast, the *dpl1 lcb3* double mutant (strain MSS207) grew slowly under all of these conditions; for example, it had a generation time of about 5 h at 30°C in rich medium, compared to 2 h for the parental strain (MSS201) and the single mutant strains (data not shown). These data suggest that one or both long-chain-base phosphates that accumulate in the double mutant impair growth.

Survival at an elevated temperature was also examined since results from several laboratories implicate sphingolipids or their metabolites in resistance to heat stress (6, 12, 14, 16, 22). Log-phase cells of the *dpl1* and *lcb3* mutant strains were 2 to 4-fold more resistant to killing at 44°C than the parental strain, while the *dpl1 lcb3* double-mutant strain was about 10-fold more resistant (Fig. 5). The correlation between increased long-chain-base phosphates and increased resistance to elevated temperature suggests that long-chain-base phosphates are components in cellular defenses against heat-induced damage.

## DISCUSSION

We have developed a simple procedure for quantifying the long-chain-base phosphates in *S. cerevisiae* cells. Using this procedure, we show for the first time that *S. cerevisiae* cells contain a barely detectable level of DHS-1-P and a higher level of PHS-1-P when grown on a fermentable carbon source at 25°C (Fig. 3A). We also show that switching cells from 25 to 37°C produces a transient eightfold increase in PHS-1-P and a

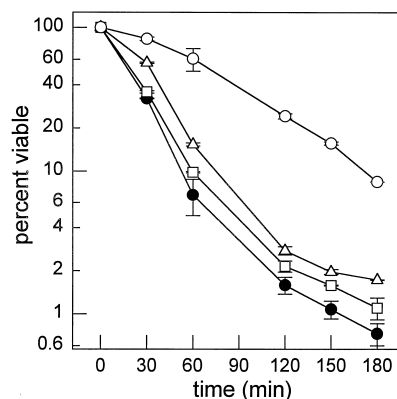


FIG. 5. Survival during heat stress. The percentage of cells able to form colonies after incubation at 44°C for the indicated times was determined for wild-type (strain MSS201; filled circles),  $\Delta dpl1$  (strain MSS204; squares),  $\Delta lcb3$  (strain MSS205; triangles), and  $\Delta dpl1 \Delta lcb3$  (strain MSS207; circles) cells. Data represent average values  $\pm$  standard deviations for two separate experiments. Some error bars are covered by the symbols. A separate isolate of the  $\Delta dpl1 \Delta lcb3$  double mutant strain gave the same result.

fivefold increase in DHS-1-P, both peaking at about 10 min and then returning to near their starting levels (Fig. 3C). In addition, analysis of mutant strains disrupted for breakdown of DHS-1-P and PHS-1-P by the *Dpl1* lyase or the *Lcb3* phosphatase pathway (Fig. 6) showed a complex, strain-specific increase of one or both long-chain-base phosphates, some of which transiently increased with heat treatment (Fig. 4). Finally, we found a correlation between accumulation of long-chain-base phosphates in mutant strains and increased survival at an elevated temperature (Fig. 5).

Sphingolipids have been implicated as signaling molecules in the heat stress response in *S. cerevisiae* (6, 12, 22). Two recent reports show that stationary-phase cells defective in *DPL1* (14) or either of the long-chain-base phosphate phosphatase genes, *LCB3* and *LBP2* (16), are more resistant to killing at elevated temperature than the parental strains. These results must be interpreted with caution, however, because the concentration of long-chain-base phosphates in stationary-phase cells was not measured. More importantly, it remains to be determined if the elevation in long-chain-base phosphates is directly responsible for increased survival at elevated temperature. It is possible that the levels of long-chain-base phosphates are elevated in mutant strains grown to stationary phase but that increased heat resistance is a pathological response to elevated levels of long-chain-base phosphates. In wild-type cells, long-chain-base phosphates may not play a direct role in heat stress resistance.

Our experiments were performed on log-phase cells, but we also find that cells deleted for *DPL1* or *LCB3* survive somewhat (two- to fourfold) better than the parental strain at an elevated temperature in (Fig. 5). We also examined a strain deleted for both *DPL1* and *LCB3*, the first time such a strain has been examined, and found that it survived 10-fold better than the parental strain (Fig. 4). Since our mutant strains had an elevated level of PHS-1-P (the *dpl1* mutant) or both PHS-1-P and DHS-1-P (the *lcb3* and the *dpl1 lcb3* mutants [Fig. 4]) and increased survival at high temperature, it appears that long-chain-base phosphates play some role in mediating resistance to heat stress. However, it is unclear whether increased heat resistance is a physiological effect or a nonphysiological effect of greatly elevated levels of long-chain-base phosphates. Increased heat resistance of the *dpl1 lcb3* double mutant may

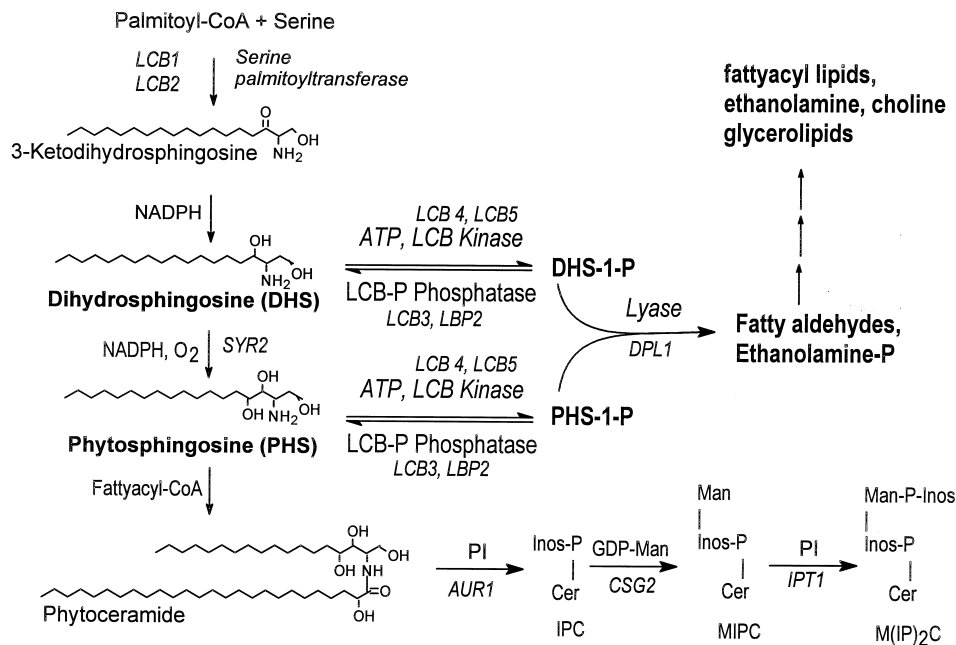


FIG. 6. Metabolism of long-chain-base phosphates in *S. cerevisiae*. Known pathway intermediates, substrates, and cofactors are indicated. Genes are in italics. Abbreviations: IPC, inositol phosphorylceramide; Man, mannose; MIPC, mannose inositol-P-ceramide; M(IP)<sub>2</sub>C, mannose-(inositol-P)<sub>2</sub>-ceramide; PI, phosphatidyl-inositol; Cer, ceramide.

in fact be an indirect effect of a reduced growth rate, since slower-growing cells survive better at high temperature (7).

If long-chain-base phosphates act as signaling molecules during heat stress, their concentration should change transiently. Our data for PHS-1-P and DHS-1-P show such a transient increase following a heat shock (Fig. 3C), suggesting that one or both of these compounds are intracellular signals. The kinetics of the increase in long-chain-base phosphates are consistent with either of them acting as signals to induce transcription of *TPS2* (Fig. 3C) and accumulation of trehalose (6), both of which occur during heat stress in *S. cerevisiae* (reference 5 and references therein).

We previously demonstrated that heat shock induces a 2 to 3-fold transient increase in the concentration of C<sub>18</sub>-DHS and C<sub>18</sub>-PHS and more than a 100-fold transient increase in C<sub>20</sub>-DHS and C<sub>20</sub>-PHS, with the maximum level occurring 10 to 15 min after the start of the heat shock (6, 12). These analyses were done by using high-pressure liquid chromatography, which can separate C<sub>18</sub> and C<sub>20</sub> molecular species. The TLC procedure described here does not allow this distinction to be made, and we do not know which species of long-chain base is present in the measured PHS-1-P and DHS-1-P. The transient increase in C<sub>18</sub>-DHS, C<sub>20</sub>-DHS, C<sub>18</sub>-PHS, and C<sub>20</sub>-PHS may provide the substrates for producing the transient increase in DHS-1-P and PHS-1-P that we observe (Fig. 3). Previous data (6, 12) along with the data presented here show that all sphingolipid intermediates examined thus far increase during a heat stress. It remains to be determined if any of these compounds are signaling molecules, and if they are, which signaling pathway(s) they regulate. One or all of these changes in sphingolipid levels may represent a physiological adaptation to heat stress, and they may not be signaling molecules. Further work is needed to decide between these alternatives.

Strain MSS207 ( $\Delta dpl1 \Delta lcb3$ ) accumulated large amounts of long-chain-base phosphates which amounted to about 2% of the total <sup>32</sup>P found in a total lipid extract (Fig. 4). This level is

about 500-fold above the level seen in wild-type MSS200 cells and may account for the reduced growth rate (5 h versus 2 h) of MSS207 cells. The slow-growth phenotype could be due to activation of a signal transduction pathway(s) that directly or indirectly regulates growth rate. But we cannot exclude the possibility that slow growth results from a nonphysiological effect of the high concentration of one of the long-chain-base phosphates on a process necessary for a normal rate of growth. In this case, the accumulation of long-chain-base phosphates represents a pathological state as seen in the sphingolipid storage diseases of mammals (19).

The accumulation of long-chain-base phosphates in cells deleted for *DPL1*, for *LCB3*, or for both genes (Fig. 4) strongly suggests that there is a flux through the metabolic pathway(s) that converts DHS and PHS to precursors for glycerolipid synthesis (Fig. 6). A direct demonstration of flux through the pathway by pulse-labeling cells with a radioactive precursor is not possible at this time for a variety of technical reasons, including the low level of PHS-1-P and DHS-1-P present in glucose-grown, log-phase cells. Pathways for breakdown of long-chain bases exist in all eucaryotes that have been examined including mammals, where sphingosine is converted to sphingosine-1-P. Our results suggest that there may be a constant flux through these pathways.

Since heat stress induces a transient accumulation of PHS-1-P and DHS-1-P (Fig. 3) in *S. cerevisiae* and since one or both of these compounds accumulate to a high level in mutant cells (Fig. 4), there must be a mechanism(s) for regulating their level in wild-type cells. Regulation is indicated also by the presence of only PHS-1-P and not DHS-1-P in *dpl1* mutant cells (Fig. 4). The lack of DHS-1-P may be due to the absence of Dpl1 lyase or the long-chain aldehyde produced by its action on DHS-1-P. Either the lyase or the aldehyde could regulate the Lcb4 and Lcb5 kinases, the Lcb3 or Lpb2 phosphatase, or both (Fig. 6). It should be possible to determine the mechanism(s) for regulating the basal level of long-chain-base phosphates.



phates and transient changes in their level, since all of the genes necessary for metabolism of long-chain-base phosphates—the lyase (*DPL1* [24]), the phosphatase (*LCB3* and *LBP2* [16, 17, 23]), and the kinase (*LCB4* and *LCB5* [21]) genes—have been identified.

Our procedure for quantifying long-chain-base phosphates in *S. cerevisiae* cells is simple, sensitive, and inexpensive and can be performed with a small quantity of cells. It should allow the level of long-chain-base phosphates to be measured under a variety of growth conditions including stressful insults in log-phase, stationary-phase, and starved cells, conditions for which there is precedent for believing that sphingolipids are essential for survival of *S. cerevisiae* cells (reference 22 and unpublished observations). The method should also be applicable to other fungi and single-cell organisms whose long-chain-base phosphates have not been analyzed.

Sphingosine and related second messengers are generally thought to be derived from breakdown of complex sphingolipids, especially sphingomyelin. For example, Swiss 3T3 fibroblasts stimulated to divide by binding of platelet-derived growth factor to its plasma membrane receptor causes hydrolysis of sphingomyelin to yield ceramide. The ceramide is cleaved by ceramidase to give sphingosine and a fatty acid, and the sphingosine is phosphorylated by sphingosine kinase to yield SPP (reviewed in references 26 and 27). The increases in PHS-1-P and DHS-1-P seen during heat shock of *S. cerevisiae* cells are not likely to be derived by breakdown of complex sphingolipids because there is no measurable breakdown (29). Also, complex sphingolipids in *S. cerevisiae* contain only PHS, not DHS, so the increase in DHS-1-P that we observe cannot be due to breakdown, unless there is an unknown pathway for converting PHS back to DHS. Current data indicate that DHS is a precursor to PHS (6, 15). Thus, *S. cerevisiae* cells may be a new paradigm for studying the generation of long-chain-base phosphates during stress responses and perhaps during other cellular processes.

#### ACKNOWLEDGMENT

This work was supported by Public Health Service grant GM41302 to R.L.L. and R.C.D.

#### REFERENCES

- Bornfeldt, K. E., L. M. Graves, E. W. Raines, Y. Igarashi, G. Wayman, S. Yamamura, Y. Yatomi, J. S. Sidhy, E. G. Krebs, S. Hakomori, and R. Ross. 1995. Sphingosine-1-phosphate inhibits PDGF-induced chemotaxis of human arterial smooth muscle cells: spatial and temporal modulation of PDGF chemotactic signal transduction. *J. Cell Biol.* **130**:193–206.
- Clarke, N. G., and R. M. C. Dawson. 1981. Alkaline O-N transacylation. *Biochem. J.* **195**:301–306.
- Cross, F. R. 1997. 'Marker swap' plasmids: convenient tools for budding yeast molecular genetics. *Yeast* **13**:647–653.
- Crowther, G. J., and D. V. Lynch. 1997. Characterization of sphinganine kinase activity in corn shoot microsomes. *Arch. Biochem. Biophys.* **337**:284–290.
- De Virgilio, C., T. Hottiger, J. Dominguez, T. Boller, and A. Wiemken. 1994. The role of trehalose synthesis for the acquisition of thermotolerance in yeast. I. Genetic evidence that trehalose is a thermoprotectant. *Eur. J. Biochem.* **219**:179–186.
- Dickson, R. C., E. E. Nagiec, M. Skrzypek, P. Tillman, G. B. Wells, and R. L. Lester. 1997. Sphingolipids are potential heat stress signals in *Saccharomyces*. *J. Biol. Chem.* **272**:30196–30200.
- Elliott, B., and B. Futcher. 1993. Stress resistance of yeast cells is largely independent of cell cycle phase. *Yeast* **9**:33–42.
- Elliott, B., R. S. Haltiwanger, and B. Futcher. 1996. Synergy between trehalose and Hsp104 for thermotolerance in *Saccharomyces cerevisiae*. *Genetics* **144**:923–933.
- Gounalaki, N., and G. Thireos. 1994. Yap1p, a yeast transcriptional activator that mediates multidrug resistance, regulates the metabolic stress response. *EMBO J.* **13**:4036–4041.
- Hanson, B. A., and R. L. Lester. 1980. The extraction of inositol-containing phospholipids and phosphatidylcholine from *Saccharomyces cerevisiae* and *Neurospora crassa*. *J. Lipid Res.* **21**:309–315.
- Heitman, J., N. R. Movva, P. C. Hiestand, and M. N. Hall. 1991. FK 506-binding protein proline rotamase is a target for the immunosuppressive agent FK 506 in *Saccharomyces cerevisiae*. *Proc. Natl. Acad. Sci. USA* **88**:1948–1952.
- Jenkins, G. M., A. Richards, T. Wahl, C. Mao, L. Obeid, and Y. Hannun. 1997. Involvement of yeast sphingolipids in the heat stress response in *Saccharomyces cerevisiae*. *J. Biol. Chem.* **272**:32566–32572.
- Kobayashi, N., and K. McEntee. 1993. Identification of *cis* and *trans* components of a novel heat shock stress regulatory pathway. *Mol. Cell. Biol.* **13**:248–256.
- Lanterman, M. M., and J. D. Saba. 1998. Characterization of sphingosine kinase (SK) activity in *Saccharomyces cerevisiae* and isolation of SK-deficient mutants. *Biochemistry* **33**:525–531.
- Lester, R. L., and R. C. Dickson. 1993. Sphingolipids with inositolphosphate-containing head groups. *Adv. Lipid Res.* **26**:253–272.
- Mandala, S. M., R. Thornton, Z. Tu, M. B. Kurtz, J. Nickels, J. Broach, R. Menzelev, and S. Spiegel. 1998. Sphingoid base 1-phosphate phosphatase: a key regulator of sphingolipid metabolism and stress response. *Proc. Natl. Acad. Sci. USA* **95**:150–155.
- Mao, C., M. Wadleigh, G. M. Jenkins, Y. A. Hannun, and L. M. Obeid. 1997. Identification and characterization of *Saccharomyces cerevisiae* dihydrosphingosine-1-phosphate phosphatase. *J. Biol. Chem.* **272**:28690–28694.
- Marchler, G., C. Schuller, G. Adam, and H. Ruis. 1993. A *Saccharomyces cerevisiae* UAS element controlled by protein kinase A activates transcription in response to a variety of stress conditions. *EMBO J.* **12**:1997–2003.
- Merrill, A. H., and C. C. Sweeley. 1996. Sphingolipids: metabolism and cell signalling, p. 309–339. *In* D. E. Vance and J. E. Vance (ed.), *Biochemistry of lipids, lipoproteins and membranes*. Elsevier Science, New York, N.Y.
- Nagiec, M. M., E. E. Nagiec, J. A. Baltisberger, G. B. Wells, R. L. Lester, and R. C. Dickson. 1997. Sphingolipid synthesis as a target for antifungal drugs. Complementation of the inositol phosphorylceramide synthase defect in strain of *Saccharomyces cerevisiae* by the *AUR1* gene. *J. Biol. Chem.* **272**:9809–9817.
- Nagiec, M. M., M. Skrzypek, E. E. Nagiec, R. L. Lester, and R. C. Dickson. 1998. The *LCB4* (*YOR171c*) and *LCB5* (*YLR260w*) genes of *Saccharomyces* encode sphingolipid long chain base kinases. *J. Biol. Chem.* **273**:19437–19442.
- Patton, J. L., B. Srinivasan, R. C. Dickson, and R. L. Lester. 1992. Phenotypes of sphingolipid-dependent strains of *Saccharomyces cerevisiae*. *J. Bacteriol.* **174**:7180–7184.
- Qie, L. X., M. M. Nagiec, J. A. Baltisberger, R. L. Lester, and R. C. Dickson. 1997. Identification of a *Saccharomyces* gene, *LCB3*, necessary for incorporation of exogenous long chain bases into sphingolipids. *J. Biol. Chem.* **272**:16110–16117.
- Saba, D. J., F. Nara, A. Bielawska, S. Garrett, and Y. A. Hannun. 1997. The *BST1* gene of *Saccharomyces cerevisiae* is the sphingosine-1-phosphate lyase. *J. Biol. Chem.* **272**:26087–26090.
- Sadahira, Y., M. Zheng, F. Ruan, S. Hakomori, and Y. Igarashi. 1994. Sphingosine-1-phosphate inhibits extracellular matrix protein-induced haptotactic motility but not adhesion of B16 mouse melanoma cells. *FEBS Lett.* **340**:99–103.
- Spiegel, S., D. Foster, and R. N. Kolesnick. 1996. Signal transduction through lipid second messengers. *Curr. Opin. Cell Biol.* **8**:159–167.
- Spiegel, S., and A. H. Merrill, Jr. 1996. Sphingolipid metabolism and cell growth regulation. *FASEB J.* **10**:1388–1397.
- Spiegel, S., A. Olivera, H. Zhang, E. W. Thompson, Y. Su, and A. Berger. 1994. Sphingosine-1-phosphate, a novel second messenger involved in cell growth regulation and signal transduction, affects growth and invasiveness of human breast cancer cells. *Breast Cancer Res. Treat.* **31**:337–348.
- Wells, G. B., R. C. Dickson, and R. L. Lester. 1998. Heat-induced elevation of ceramide in *Saccharomyces cerevisiae* via *de novo* synthesis. *J. Biol. Chem.* **273**:7235–7243.
- Yamamura, S., Y. Sadahira, F. Q. Ruan, S. Hakomori, and Y. Igarashi. 1996. Sphingosine-1-phosphate inhibits actin nucleation and pseudopodium formation to control cell motility of mouse melanoma cells. *FEBS Lett.* **382**:193–197.
- Zhang, H., N. N. Desai, A. Olivera, T. Seki, G. Brooker, and S. Spiegel. 1991. Sphingosine-1-phosphate, a novel lipid, involved in cellular proliferation. *J. Cell Biol.* **114**:155–167.
- zu Heringdorf, D. M., C. J. van Koppen, and K. H. Jakobs. 1997. Molecular diversity of sphingolipid signalling. *FEBS Lett.* **410**:34–38.